UNSYS digital

Journal of Unmanned System Technology

2D Quasi-Steady Flow Simulation of an Actual Flapping Wing

Lung Jieh Yang[†], H.-L. Huang[†], J.-C. Liou[†], B. Esakki[‡], and U. Chandrasekhar[§]

[†]Tamkang University, Tamsui, Taiwan

[‡]VelTech Dr. RR Dr. SR Technical University, Avadi, Chennai, India

[§]ESCI-Autonomous Organ of the Institution of Engineers, Hyderabad, India

***Abstract*—**This paper deals about the dynamic behavior of flapping wing with an aid of stereo photography measurement using charge coupled device (CCD) camera. The three dimensional (3D) flapping motion was captured and coordinates are measured with the specific markers on the wing. The curved surface fitting was obtained from the 3D discrete coordinates using SURFER software. Consequently, a two dimensional (2D) cross section of flapping motion of the wing surface is sliced from 3D mesh. It was used further for the quasi-steady state computational fluid dynamics (CFD) simulation in Fluent. Utilizing two adjacent 2D trajectories, the upwind direction of flow filed was computed in this study. The computed dynamic velocity was considered to be input for the CFD analysis. The velocity and pressure distribution due to quasi-steady state flapping motion is observed in Fluent. The unsteady lift coefficient was obtained which was compared with experimental results from the wind tunnel. It was observed that, both theoretical and experimental results shows similar trend to validate the assumptions considered in the study.

***Keywords*—**Flapping, micro-air-vehicle (MAV), stereo photography, computation fluid dynamics (CFD), quasi-steady.

I. INTRODUCTION

FLAPPING wing flight was one of the complex flights found in nature and over 10,000 birds and bats flaps their wings for locomotion [1]. The study on the aerodynamics of flapping wing micro-air-vehicle (MAV) plays vital role to understand its behavior. Especially two and three dimensional flapping wing motions are critical area for scientific understanding. In the low Reynolds number regimes of MAVs of the order 10^4–10^5, the fixed wing aerodynamic performance drops while flexible flapping wing effectively propels. The researchers have realized that steady state aerodynamics may not capture the flying characteristics or forces present in the flapping wing motion [2]. In order to understand the aerodynamics behavior at various wind conditions, unsteady flow study is necessary. Various researchers [3-13] studied the unsteady aerodynamics of flapping wing vehicles. Recently, Moelyadi et al. [14] conducted the quasi-steady state and unsteady state analysis using computational fluid dynamics (CFD). However, they have not considered real-time data of upwind direction in their analysis. The present study focuses on obtaining the proper upwind direction and the magnitude of the uniform flow for the quasi-steady CFD.

Corresponding author: Lung Jieh Yang (e-mail: ljyang@mail.tku.edu.tw).
This paper was submitted on November 15, 2013; revised on January 09, 2014; and accepted on February 24, 2014.

The MEMS research group at Tamkang University has devoted to the development of palm-size flapping MAVs for many years [15-19]. Electrical-discharge-wire-cutting (EDWC) technology was first used to fabricate the 4-bar linkage flapping mechanism of a palm-size biomimetic MAV "Golden Snitch" with the total mass of 6g in 2009 [15]. In 2012, the fabrication of a polymeric "Golden Snitch" is successful implemented, and the precision injection molding technique shows its feasibility in commercial realization and mass production of this MAV [16]. While studying the effects of wing configuration and stiffness on the aerodynamic performance of "Golden Snitch" in wind-tunnel testing, a well-designed flapping wing foil made by PET is proposed [17]. The modified MAV "Golden Snitch" prolongs its flight endurance record to 8 min.

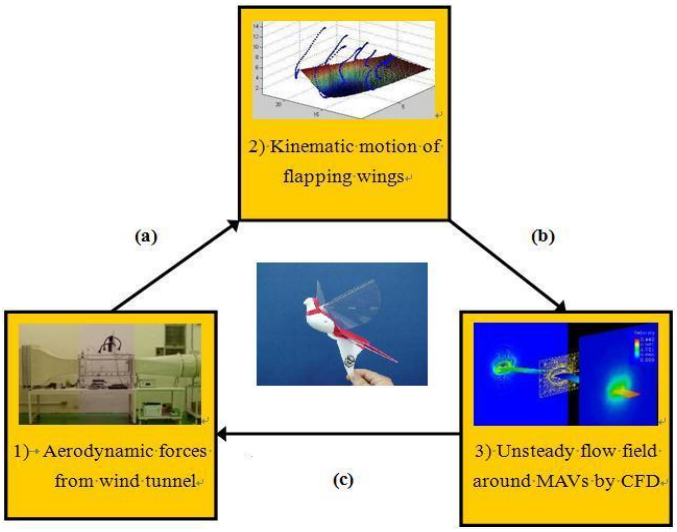

Figure 1 The triangle research framework of flapping MAVs "Golden Snitch" at Tamkang University: (a) Comparing the theoretical trajectory with the stereo image trajectory; (b) Providing the dynamic wing boundary for CFD simulation; (c) Comparing the lift/thrust with the wind tunnel data.

In 2012, the figure-8 trajectories of the MAVs' wing tips were confirmed by their proper function of the carbon-fiber wing frames and the parylene wing skin [18]. The authors moreover constructed the research framework in **Figure 1** which necessitates the numerical computation and investigation of the unsteady flapping flow field using CFD.

In most CFD flow calculations around flapping wings, the real time wing kinematics is prescribed and the velocity of the wing is computed by differentiating the wing kinematics in time. Thus, the wing velocities in the three axes directions are implemented for CFD calculation [19] or other numerical methods [20]. However, when we conventionally used the captured 3D coordinates of the time-varying wing trajectory from the stereo photography, it was hard to prescribe and transform the real 3D wing profiles into well-posed functions to act as the user-defined functions (UDF), e.g. in Fluent. Our previous work in [21] therefore presented the quasi-steady CFD to avoid using the UDF in some CFD software. Another advantage of the quasi-steady CFD over the exactly unsteady CFD is that the consumption of time is very less.

The time-varying lift data of 15.4 Hz flapping from the quasi-steady CFD results seems to have the similar changing trend with the wind tunnel data in the conclusion of [21]. However, the computed quasi-steady lift coefficient is actually improper due to the crude inlet boundary conditions. In our previous work does not consider the real time data of upwind direction for the numerical simulation. Hence, in this work we tried to artificially modify the upwind boundary conditions by the captured wing kinematics for the quasi-steady CFD analysis of flapping MAVs.

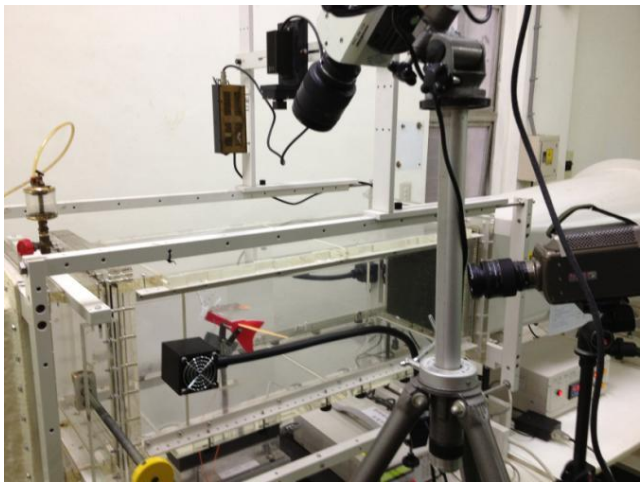

Figure 2 Capturing flapping motion

II. Flapping Motion Sensing and Post Processing

In order to measure the flapping motion of wing, two high speed stereo vision CCD cameras were used which are placed at different angles so that the discrete 3D coordinates of the complete flapping wing foil motion will be measured [5] which is shown in **Figure 2**.

The captured 3D coordinates were transferred into MATLAB and the corresponding flapping motion of the foil was visualized. **Figure 3** shows the deforming profiles of the flapping membrane wing corresponding to every 60° phase angle of a wing beating cycle which was obtained by the driving voltage of 3.7 V.

Figure 3 confirms the flapping motion of wing as in the case of real time measurement using CCD camera. To conduct unsteady state CFD analysis of the flapping wing, the real time dynamics boundary conditions are necessary. In view of this, the curved surface fitting is obtained from the 3D discrete coordinates using SURFER software. The modified Sheppard's method was used to interpolate the coordinates to obtain the 3D mesh. From the 3D mesh of motion of the flapping wing, a 2D time varying trajectory was sliced at the middle of the 3D mesh which is shown in **Figure 4**. The reasons for selecting the 2D wing section at the 50% wing span are addressed as below: (1) The 2D wing section cannot be chosen at the wing tip because of 3D trailing vortex which are beyond the capability of 2D flow simulation. (2) The wing root or the centerline of the flapping wing is also not a good candidate for the 2D wing section because no more flapping motion can be observed in that region. Based on the above two reasons, the authors selected the chord-wise trajectory at 50% of wing span which has the classical feature of flapping flow pattern for a 2D case to achieve.

Figure 5(a) shows the tracing of wing motion in the upstroke and **Figure 5(b)** depicts the down-stroke wing beat. These trajectories are further considered to determine the upwind direction and magnitude. In order to consider the dynamic boundary conditions for unsteady state flow analysis, the two adjacent 2D trajectories were considered to explain the upwind direction and magnitude of velocity. As shown in **Figure 6**, utilizing the two adjacent 2D trajectory coordinates for the time interval of Δt, instantaneous flapping velocity (V_x, V_y) of the aerofoil leading edge due to the flapping motion was determined which will be further used as the boundary conditions for quasi-steady state CFD analysis.

$$V_x = \frac{X_2 - X_1}{\Delta t} \quad (1)$$

$$V_y = \frac{Y_2 - Y_1}{\Delta t} \quad (2)$$

III. Quasi-Steady State Flow Analysis and Validation

A. Numerical Study Using CFD

The sliced 2D profile was considered to perform the quasi steady state flow analysis. In order to improve the accuracy and also save time, a fine mesh was created by forming the circle around the 2D aero foil and also outside the circle, a coarse mesh was considered. The uniform velocity of 3 $m.s^{-1}$ and also the instantaneous flapping velocity obtained from the 2D profile in equations (1) and (2) were given as boundary conditions in Fluent to perform CFD analysis. As the flapping wing beat cycle is divided into 70 segments, for each segment the boundary conditions were varied and corresponding CFD analysis was carried out until the solution converges.

The detailed setup or procedure of the Fluent is as follows:

(1) Define the whole computation domain of 0.6 m × 0.3 m and read the 2D wing section coordinates corresponding to a certain time step into Gambit software;
(2) Define a circle with a diameter of 0.2 m around the flapping wing section;
(3) Generate coarse mesh of 3,350 triangular grids outside the

circle and fine mesh of 2,000-4,500 squared grids inside the circle;

(4) Command the "velocity-inlet" by equations (1)-(2) at the left boundary and command other boundaries with "outflow";

(5) Select the "2nd-order upwind" scheme to solve the steady state flow field for each time step until the cumulative error converges to 10^{-4};

(6) Output the pressure field, velocity field and the lift coefficient for each time step up to the complete flapping cycle.

The velocity contour for the aforementioned boundary conditions and for the flapping frequency of 15 Hz is shown in **Figure 7**. It is evident from the figures that, the flow pattern is bended and also able to visualize the flapping phenomena of down-stroke and upstroke, respectively.

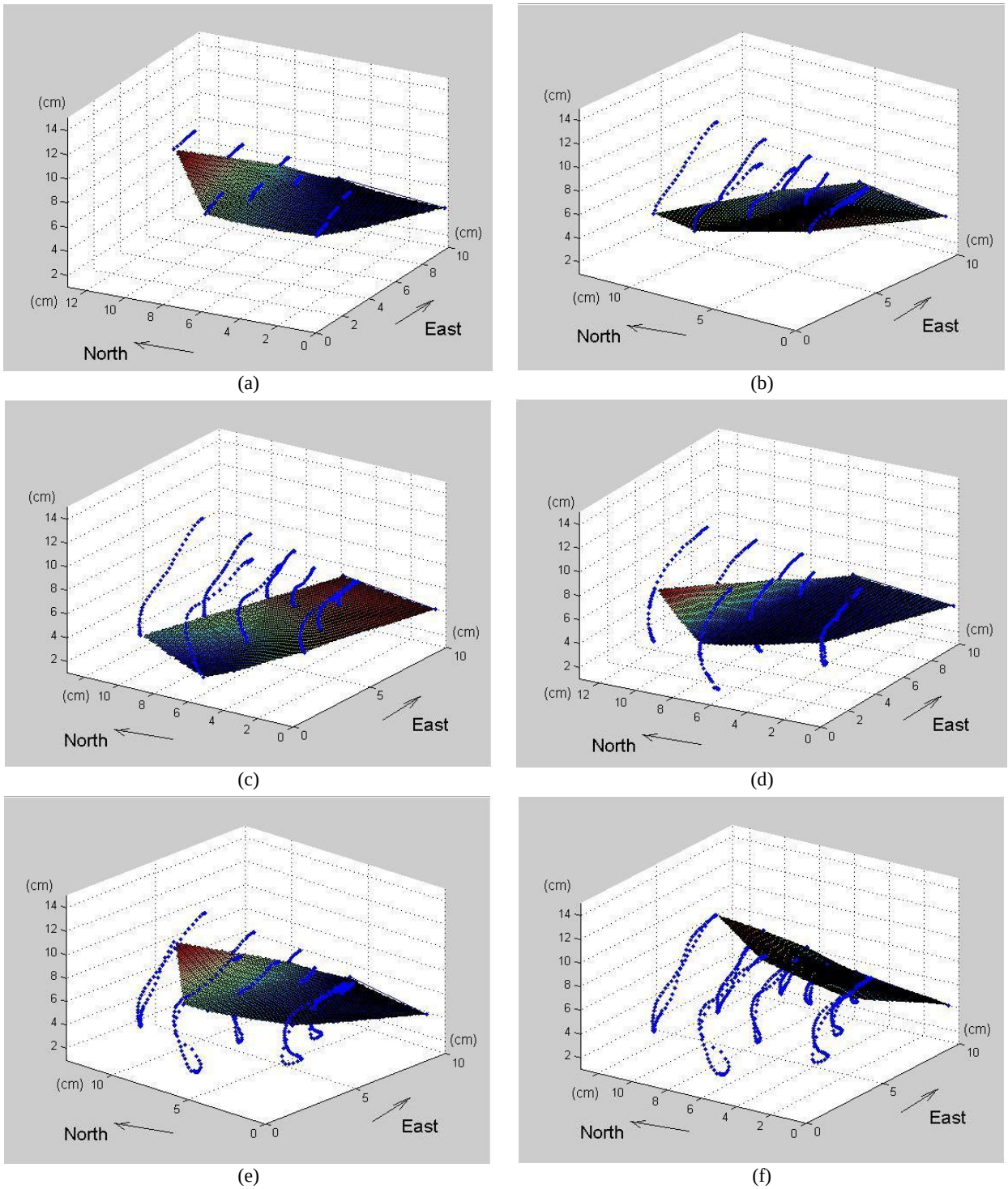

Figure 3 The deforming profiles of the flapping membrane wing corresponding to every 60° phase angle of a wing beating cycle; driving voltage=3.7V [21]: (a) 60°; (b) 120°; (c) 180°; (d) 240°; (e) 300°; (f) 360°.

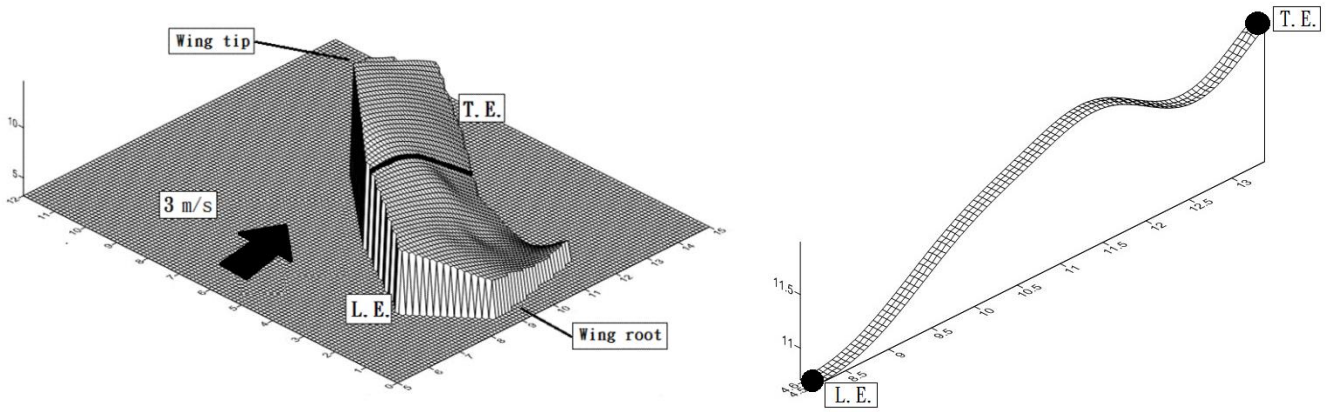

(a) (b)

Figure 4 (a) 3D mesh fitting by SURFER; (b) 2D slice of the flapping motion.

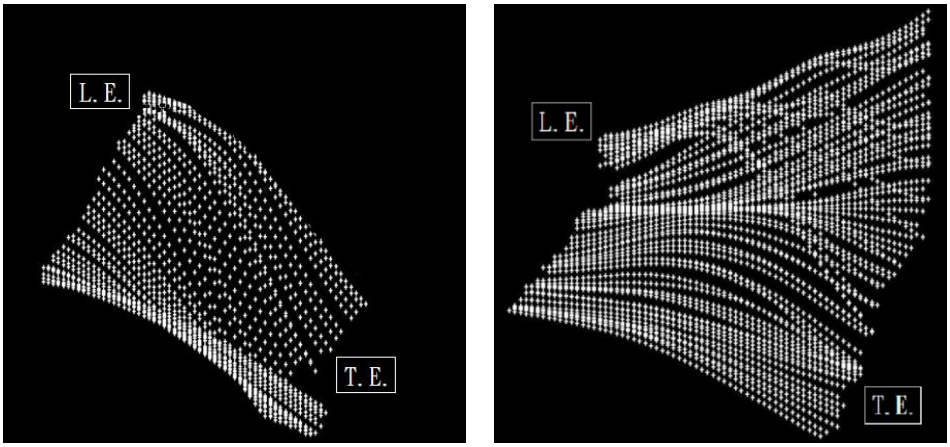

(a) (b)

Figure 5 (a) Upstroke flapping (b) downstroke flapping

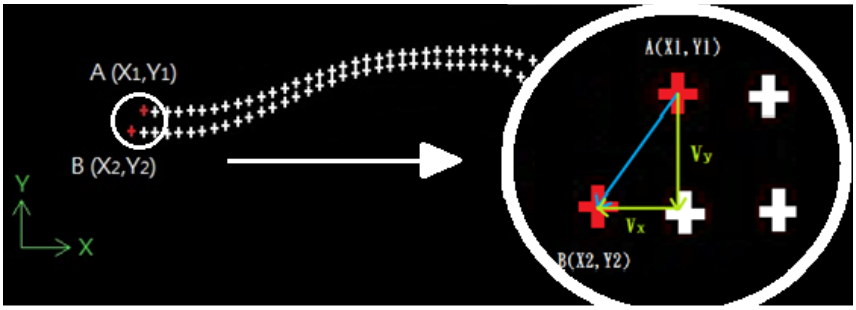

Figure 6 Two trajectory and velocity calculation of the leading edge.

B. Lift Force Validation

To compare the experimental data of the lift force, quasi-steady state lift coefficient was obtained from the CFD analysis was taken into account. The **Figure 8** shows the experimental setup for the measurement of lift force using wind tunnel subject to one flapping cycle. **Figure 9(a)** shows the trend of lift force coefficient for the flapping frequency of 15 Hz which is almost similar pattern of experimental results as shown in **Figure 9(b)** obtained from the wind tunnel. Even though it's hard to combine together a small difference in time scale, the authors still trimmed **Figure 9(a)** and **(b)** into a full cycle for easy comparison. In general, the measured force from the wind tunnel always includes inertial force, and the CFD provides only the aerodynamic force [20, 22]. This is also the reason why these two sets of data differ a lot during the upstroke reversal or the down-stoke reversal. However, the authors cannot subtract the inertia force from the wind-tunnel data without the vacuum testing chamber at the current stage and this will be considered in our future work.

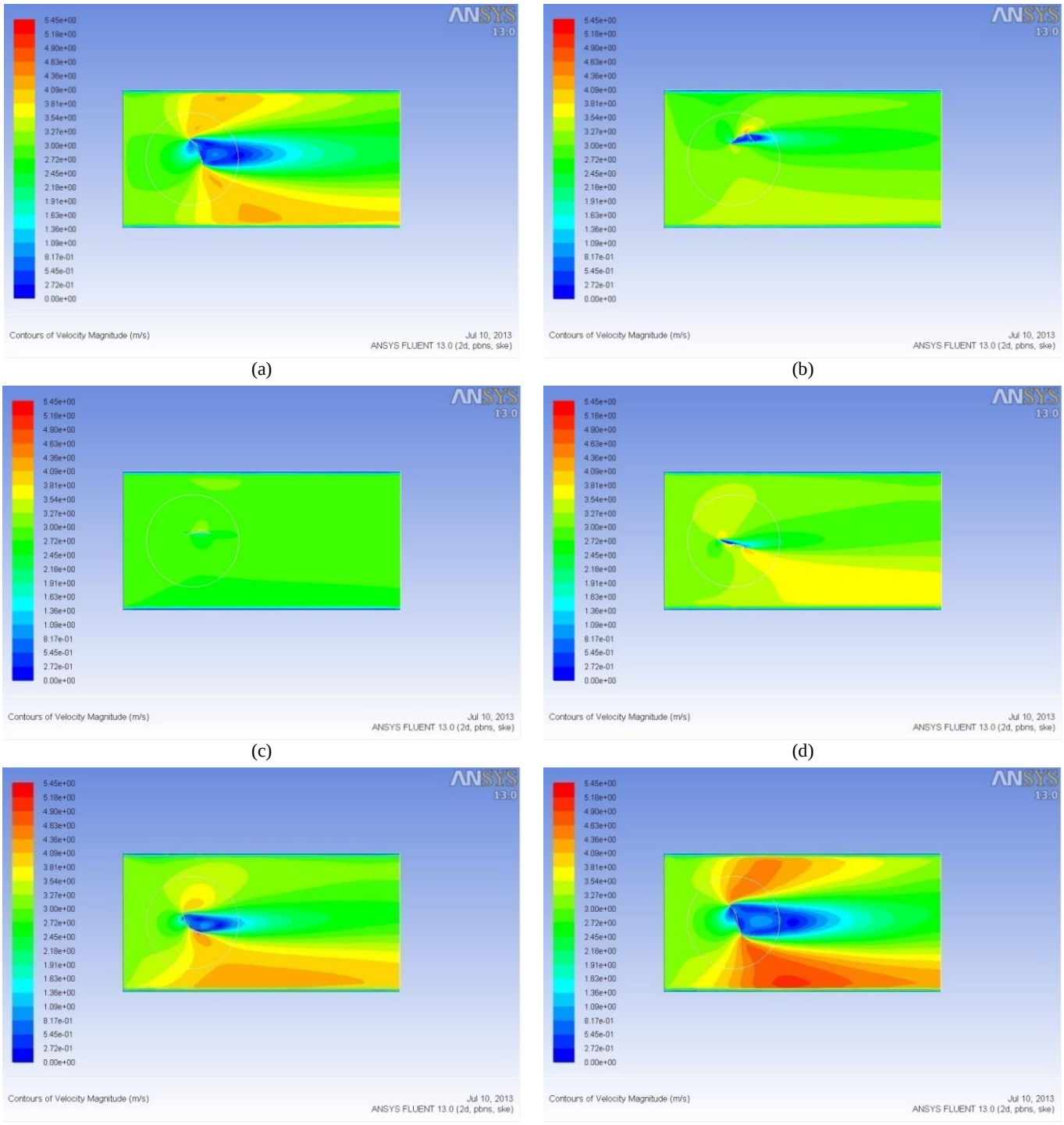

Figure 7 Equi-velocity contour (unit: ms^{-1}) of the flapping flow field operated at 3.7V; wingbeat frequency is 15Hz; freestream velocity is $3ms^{-1}$; (a)-(c) denoting the upstroke and (d)-(f) denoting the down-stroke in a flapping cycle.

Figure 8 Wind tunnel experiments

IV. CONCLUSIONS

The proposed work determines the direction of upwind from the real time flapping motion of the wing which is considered to be an input to the CFD analysis. Capturing of 3D flapping motion of the wing using stereo vision camera and slicing into 2D profile provided the path for the quasi-steady state CFD analysis. The CFD analysis provided greater insight for the up and down stream velocity of the flapping wing for the real time boundary conditions. The conducted CFD analysis also reveals that the determination of lift coefficient would ensure the lift force characteristics as like the real time measurement using wind tunnel. In future, 3D flapping motion and corresponding unsteady flow simulation will be carried out.

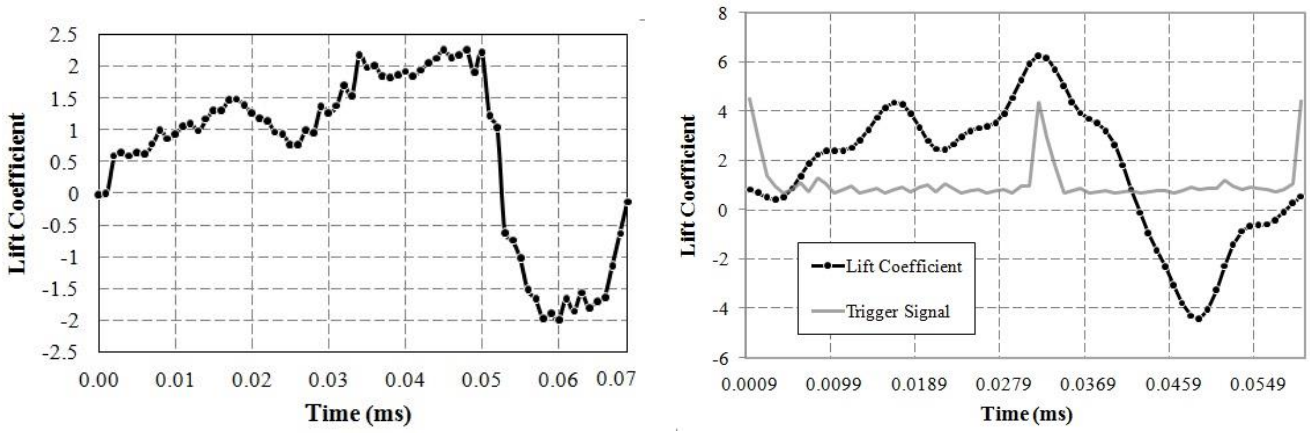

(a) (b)

Figure 9 The unsteady lift force information: (a) the lift coefficient history of a flapping cycle predicted by this work; (b) the experimental lift data of the "Golden Snitch" in a wind tunnel subject to one flapping cycle [17].

ACKNOWLEDGMENT

The authors give the heartfelt thanks for the financial support of the National Science Council of Taiwan (project numbers NSC-101-2632-E-032-001-MY3 and NSC 102-2923-E-032-001-MY3).

REFERENCES

[1] K.P. Dial, "An inside look at how birds fly: experimental studies of the internal and external processes controlling flight," 1994 Report the Aerospace Profession, 38th Symposium Proceedings, The Beverly Hilton, Beverly Hills, CA, 1994.

[2] S. Ho, H. Nassef, N. Pornsinsirirak, Y.-C. Tai, C.-M. Ho, "Unsteady aerodynamics and flow control for flapping wing flyers," *Progress in Aerospace Sciences*, volume 39, 2003, pp. 635–681. CrossRef

[3] M.H. Dickinson and K.G. Gotz, "Unsteady aerodynamic performance of model wings at low Reynolds numbers," *Journal of Experimental Biology*, volume 174, 1993, pp. 45–64.

[4] C.P. Ellington, C. van Den Berg, A.P. Willmott, and A.L.R. Thomas, "Leading-edge vortices in insect flight," *Nature*, volume 384, 1996, pp. 626–30. CrossRef

[5] T. Maxworthy, "Experiments on the Weis-Fogh mechanism of lift generation by insects in hovering flight. Part 1. Dynamics of the fling," *Journal of Fluid Mechanics*, volume 93, 1979, pp. 47–63. CrossRef

[6] M. Sun and J. Tang, "Unsteady aerodynamic force generation by a modelfruit fly wing in flapping motion," *Journal of Experimental Biology*, volume 205, 2002, pp. 55–70.

[7] S. Ho, "Unsteady aerodynamics and adaptive flow control of micro air vehicles," Ph.D. dissertation, University of California, Los Angeles, 2003.

[8] K. Danesh and Tafti, "Unsteady aerodynamics of a flapping wing for mico air vehicle (MAV) applications," *Proceedings of the 37th National & 4th International Conference on Fluid Mechanics and Fluid Power*, pp. 1-11, 2010.

[9] M.S. Vest and J. Katz, "Unsteady aerodynamic model of flapping wings," *AIAA Journal*, volume 34, number 7, 1996, pp. 1435-1440. CrossRef

[10] M.A. Moelyadi and G. Sachs, "CFD-based determination of dynamic stability derivatives in yaw for a bird," *Journal of Bionic Engineering*, volume 4, number 4, 2007, pp. 201-208. CrossRef

[11] G. Sachs and M.A. Moelyadi, "CFD-based determination of aerodynamic effects on birds with extremely large dihedral," *Journal of Bionic Engineering*, volume 7, number 1, 2010, pp. 95-101. CrossRef

[12] Z. J. Wang, "Vortex shedding and frequency selection in flapping flight," *Journal of Fluid Mechanics*, volume 410, 2000, pp.323-341. CrossRef

[13] Z.J. Wang, "The role of drag in insect hovering," *Journal of Experimental Biology*, volume 207, 2004, pp. 4147-4155. CrossRef

[14] M.A. Moelyadi and G. Sachs, "Unsteady aerodynamics of flapping wing of a bird," *J. Eng. Technol. Sci.*, volume 45, number 1, 2013, pp. 47-60.

[15] L.J. Yang, C.K. Hsu, H.C. Han, and J.M. Miao, "A light flapping micro-aerial-vehicle using electrical discharge wire cutting technique,"

Journal of Aircraft, volume 46, number 6, 2009, pp. 1866-1874. CrossRef

[16] L.J. Yang, C.Y. Kao, and C.K. Huang, "Development of flapping ornithopters by precision injection molding," *Applied Mechanics and Materials*, volume 163, 2012, pp. 125-132. CrossRef

[17] L.J. Yang, A.F. Kuo, and C.K. Hsu, "Wing stiffness on light flapping MAVs," *Journal of Aircraft*, volume 49, number 2, 2012, pp. 423-431. CrossRef

[18] L.J. Yang, "The micro-air-vehicle Golden Snitch and its figure-of-8 flapping," *Journal of Applied Science and Engineering*, volume 15, number 3, 2012, pp. 197-212. C

[19] L.T.K. Au, V.H. Phan, A. Budiyono, and H.C. Park, "Dynamic stability in vertically flying insect-mimicking flapping wing system," The 10th International Conference on Ubiquitous Robots and Ambient Intelligence, Jeju, South Korea, October 30-November 2, 2013, pp. 27-28.

[20] Q.T. Truong, Q.V. Nguyen, V.T. Truong, H.C. Park, D.Y. Byun, and N.S. Goo, "A modified blade element theory for estimation of forces generated by a beetle-mimicking flapping wing system," *Bioinsp. Biomim.*, volume 6, number 3, 2011, 036008. CrossRef

[21] L. J. Yang, F. Y. Hsiao, W. T. Tang, and I. C. Huang, "3D flapping trajectory of a micro-air-vehicle and its application to unsteady flow simulation," *International Journal of Advanced Robotic Systems*, volume 10, 2013, paper no. 264.

[22] Q.V. Nguyen, H.C. Park, N.S. Goo, and D. Byun, "Aerodynamic force generation of an insect-inspired flapper actuated by a compressed unimorph actuator," *Chinese Science Bulletin*, volume 54, 2009, pp. 2871-2879. CrossRef